Atomic ordering in $xZrO_2 \cdot (1-x)\,SiO_2$ xerogels (x=0.3, 0.5) by X-ray diffraction and reverse Monte Carlo simulations

O. STACHS, Th. GERBER, V. PETKOV*
Fachbereich Physik, Universität Rostock, Universitätsplatz 3, 18051 Rostock, Germany

Atomic distribution functions for $xZrO_2 \cdot (1-x)\,SiO_2$ xerogels ($x = 0.3, 0.5$) have been obtained by X-ray diffraction experiments. Three dimensional structure models that closely reproduce the experimental structural data have been constructed by reverse Monte Carlo simulations. The model results suggest that the investigated xerogels do not exhibit any characteristics of a phase segregation and have a homogeneous structure at the atomic scale. In particular, the local atomic ordering in $0.5ZrO_2 \cdot 0.5SiO_2$ xerogels heat treated to 770 K has been found to be similar to that in crystalline $ZrSiO_4$. The question as to why a phase segregation occurs on the crystallization of $xZrO_2 \cdot (1-x)\,SiO_2$ xerogels ($x - 0.3, 0.5$) has been addressed.

I. Introduction

ZrO_2-containing silicates are important technological materials due to their excellent resistance to alkali corrosion and their low thermal expansion values [1–4]. The preparation of these materials by the conventional solid state reaction route which involves the mixing of SiO_2 and ZrO_2 oxides followed by a thermal treatment at elevated temperatures requires the use of high temperatures if the synthesis is to be fully completed. Thus alternative routes to the synthesis of these materials have been investigated and developed. In this respect, sol–gel technology has proved to be rather successful. It has been found that by employing the sol–gel route ZrO_2–SiO_2 amorphous materials and gels, can be produced over quite a wide composition range at almost ambient temperatures [5–8]. By subjecting these amorphous materials to a further thermal treatment ZrO_2–SiO_2 glasses, crystalline powders, thin layers and other technological materials have been easily produced [9–12]. Since the morphology and the structure-dependent properties of the materials obtained via the sol–gel route are significantly influenced by the structural characteristics of the parent gel, a number of studies have dealt with the atomic-scale structure of ZrO_2–SiO_2 gels. In these studies emphasis has been placed on revealing the distribution of Zr and Si atoms in the amorphous structure. Evidence for the presence of Zr–O–Si bonds has been found by Raman and IR spectroscopy experiments [9, 13] which has been considered as an indication that the distribution of Si and Zr atoms in the ZrO_2–SiO_2 gels investigated is more or less uniform on the atomic scale. No evidence for the formation of clusters rich in Zr atoms has been found by extended-X-ray absorption fine structure (EXAFS) experiments [14]. However these ZrO_2–SiO_2 gels and glasses obtained from the gels have been observed to always decompose into ZrO_2 and SiO_2 when heated at high enough temperatures. An inherent tendency of the Zr atoms towards clustering, even at low concentrations, has been suggested by the results of molecular dynamics simulations on the ZrO_2–SiO_2 system [15]. These findings may be taken as an indication that Si and Zr atoms are not quite uniformly distributed in the ZrO_2–SiO_2 gels. Thus it seems that no clear answer to the question: what is the atomic-scale distribution of Zr and Si atoms in ZrO_2–SiO_2 gels? can be obtained on the basis of the structural information collected to date. It is the purpose of the present study to clarify the situation by carrying out a new structural investigation on $xZrO_2 \cdot (1-x)\,SiO_2$ xerogels ($x = 0.3, 0.5$), using X-ray diffraction techniques. Three dimensional structural models that closely reproduce the experimental data have been constructed by reverse Monte Carlo simulations. The structural characteristics of the models have been analysed in detail in order to reveal the spatial distribution of Si and Zr atoms. The question: why do ZrO_2–SiO_2 gels decompose into ZrO_2 and SiO_2 upon crystallization? is addressed.

2. Experimental procedures

2.1. Sample preparation

$xZrO_2 \cdot (1-x)\,SiO_2$ xerogels ($x = 0.3, 0.5$) were prepared by the controlled hydrolysis and condensation of tetraethylorthosilicate, $Si(OC_2H_5)_4$ (TEOS), and a 70% solution of zirconium η-propoxide in propanol.

* On leave from Department of Solid State Physics, Sofia University, Sofia – 1126, Bulgaria.

0022–2461

Ethanol (C_2H_5OH), and hydrochloric acid (HCl) were used as the solvent and as a catalyst, respectively. Since the reaction rates of TEOS and η-propoxide alkoxides differ, partial hydrolysis procedures were applied in order to produce the sol. This method has been previously applied to successfully produce TiO_2–SiO_2 gels [16, 17]. The production of the sol occured at room temperature in the following manner: at first all the TEOS used was dissolved in half of the ethanol and stirred while the water and acid were added in drops. After stirring the resulting solution for 5 min the zirconium η-propoxide, dissolved in the rest of the ethanol, was added in drops under continuous stirring. With the following ratios of the parent products used: ethanol/alkoxides = 90, water/alkoxides = 10 and acid/alkoxides = 0.25 the gelation of the sol was completed after ~700 h. The wet gels were dried at 320 K in air and further heated at 370 K for 2 h. The thus obtained xerogels were ground into fine powders which were probed using X-ray diffraction techniques.

2.2. X-ray diffraction investigations

The X-ray diffraction experiments were carried out using the synchrotron radiation beamline 7/2 at the Stanford Synchrotron Radiation Laboratory, USA. The experiments were performed in a symmetrical transmission geometry ($\Theta - 2\Theta$ mode) in steps of 0.01°. The white synchrotron beam was monochromated by a double crystal Si(400) monochromator. The diffracted X-ray photons were detected by a nitrogen cooled Ge solid state detector coupled to a 4-channel analyser which separated the incoherent scattering from the coherent scattering and also reduced the overall background scattering. The 17 keV X-rays ($\lambda = 0.0708$ nm) selected by the monochromator were used to collect high quality diffraction data up to 1.4 nm^{-1} (130° in 2Θ). After applying the appropriate correction factors as described in references [18–20] the coherently scattered intensities, $I^{coh}(q)$, were extracted from the measured diffraction spectra and the corresponding structure factors, $S(q)$, defined as follows:

$$S(q) = 1 + [I^{coh}(q) - \sum c_i f_i^2(q)]/\sum c_i f_i(q)]^2 \quad (1)$$

were calculated. Here c_i and $f_i(q)$ are the atomic concentration and the atomic scattering factor of the atomic species of type i(i = Zr, Si, O), respectively, and q is the amplitude of the scattering(wave) vector ($q = 4\pi\sin(\Theta/\lambda)$). By carrying out a Fourier transformation the corresponding reduced atomic distribution functions, $G(r)$,

$$G(r) = 4\pi r[\rho(r) - \rho_0]$$
$$= (2/\pi)\int_{q=0}^{q_{max}} q[s(q) - 1]\sin(qr)\, dq \quad (2)$$

where $\rho(r)$ and ρ_0 are the local and the average atomic number densities as well as a distance in real space, respectively, were calculated.

Structure factors obtained in this way and corresponding atomic distribution functions for the two investigated xerogels are shown in Figs 1 and 2,

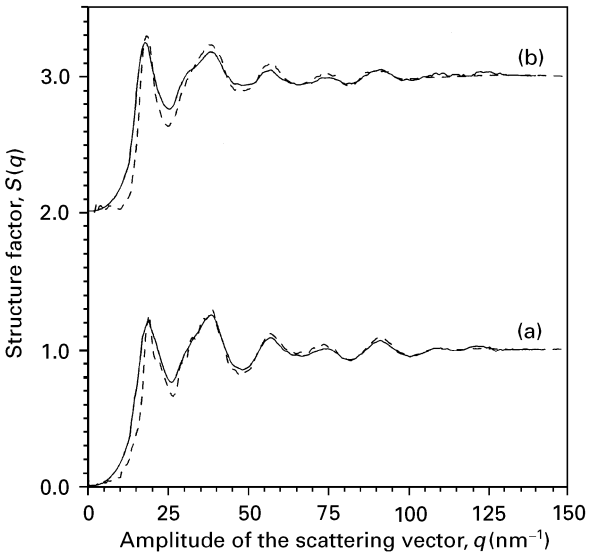

Figure 1 Structure factors, $S(q)$, for (a) $0.5ZrO_2 \cdot 0.5\,SiO_2$ and (b) $0.3ZrO_2 \cdot 0.7SiO_2$ xerogels. Key: (—) experimental data, (- - - -) RMC results.

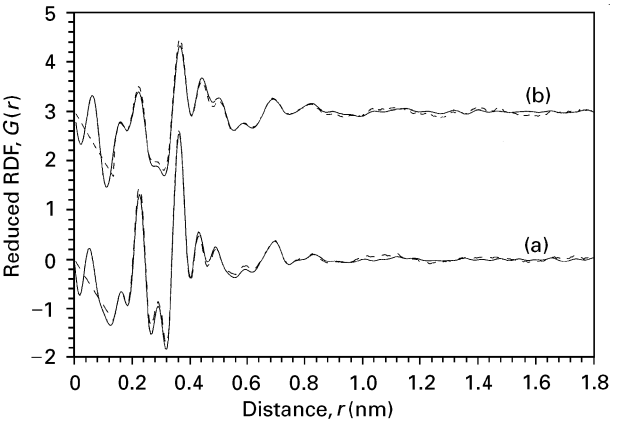

Figure 2 Reduced atomic distribution functions for (a) $0.5ZrO_2 \cdot 0.5\,SiO_2$ and (b) $0.3ZrO_2 \cdot 0.7\,SiO_2$ xerogels. Key: (—) experimental data; (- -) RMC fits.

respectively. As can be seen in Fig. 1 the experimental structure factors are composed of low amplitude peaks the first of which is centred at approximately 18.5 nm^{-1}. The relatively low amplitude of the first peak in both structure factors indicates that no well-defined long-range atomic correlations are present in the investigated xerogels. This observation is confirmed by the fact that no pronounced peaks are present in the corresponding atomic distribution functions at real space distances longer than 1.0–1.2 nm (see Fig. 2). The first few physically sensible peaks in both atomic distribution functions are centred at approximately 0.16, 0.225, 0.285, 0.36, 0.43 and 0.49 nm. Amongst these peaks, the one centred at 0.36 nm has the highest amplitude. By referring to available structure data for ZrO_2–SiO_2 materials and taking into account the ionic radii of Si, Zr and O it was reasonable to attribute the first peak in the experimental atomic distribution functions at 0.16 nm to the first neighbour Si–O atomic pairs present in the investigated xerogels. The second peak at 0.235 nm was attributed to the first neighbour Zr–O atomic pairs, the

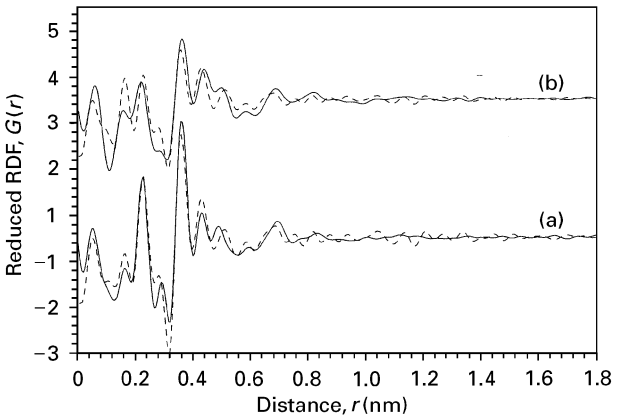

Figure 3 Comparison between (—) experimental and (- - -) model atomic distribution functions for (a) $0.5ZrO_2 \cdot 0.5\,SiO_2$ and (b) $0.3ZrO_2 \cdot 0.7\,SiO_2$ xerogels. The model atomic distribution functions are superpositions of properly weighed experimental atomic distribution functions for the SiO_2 and ZrO_2 xerogels.

small amplitude third peak at 0.285 nm – to the first neighbour Zr–Si atomic pairs and the highest amplitude peak at 0.36 nm to the first neighbour Zr–Zr and Si–Si atomic pairs. This preliminary analysis of the experimental atomic distribution functions was also supported by the observation that the amplitude of the peak at 0.162 nm, attributed to Si–O atomic correlations, increases while the amplitudes of the peaks at 0.225, 0.285 and 0.362 nm, attributed to Zr involving atomic correlations, decrease in line with the change of the Si/Zr ratio (see Fig. 2). The next step in the preliminary analysis of the experimental data was to check whether the investigated xerogels could be considered as a mixture of SiO_2 and ZrO_2 rich phases i.e., to check if the Zr and Si atoms are not fully homogeneous at the atomic scale. To do so we compared the experimental atomic distribution functions for the $xZrO_2 \cdot (1-x)\,SiO_2$ xerogels ($x = 0.3, 0.5$) with model ones representing a properly weighed superposition of experimental atomic distribution functions for ZrO_2 and SiO_2 xerogels.

The two experimental distribution functions for the ZrO_2 and SiO_2 xerogels were obtained and processed in the same way as those for the ZrO_2–SiO_2 xerogels discussed in the present study. The results of the comparison are shown in Fig. 3. As can be seen in the figure the calculated model atomic distribution functions fail to reproduce the experimental data especially in the region of r values between 0.16–0.6 nm where, our preliminary analyses suggest that the first neighbour atomic correlations in $xZrO_2 \cdot (1-x)SiO_2$ xerogels ($x = 0.3, 0.5$) should occur. This observation suggested that the investigated xerogels are not a mixture of ZrO_2 and SiO_2 rich phases and this result prompted us to search for other models that better reproduce the experimental data. Such models were successfully constructed by reverse Monte Carlo simulations, as will now be discussed.

3. Reverse Monte Carlo simulations on $xZrO_2 \cdot (1-x)\,SiO_2$ xerogels ($x = 0.3, 0.5$)

The reverse Monte Carlo method (RMC) used in the modelling of disordered structures involves random movements of atoms placed in a simulation box with periodic boundary conditions. Moves are accepted if the difference between the calculated model and experimentally derived structure-sensitive data, (usually given in terms of structure factors and atomic distribution functions), is reduced. The process is repeated until an almost perfect fit to the experimental data is achieved. The resulting three dimensional atomic configuration is considered to be a statistically representative model of the material under study. From the configuration constructed important structural characteristics such as partial atomic distribution functions, co-ordination numbers and distances are determined by geometrical analyses of the atomic coordinates [21–24].

The present simulations on the $xZrO_2 \cdot (1-x)\,SiO_2$ xerogels were carried out on atomic configurations of 4200 atoms placed in cubic boxes of appropriate edge lengths.

During the simulations the random movements of the atoms from the model atomic configurations were limited by "cut-off" distances which prevented the atoms from approaching each other to an unrealistically close distance. The following "cut-off" distances of 0.14, 0.19, 0.21, 0.265, 0.335 and 0.340 nm estimated from all the available structure data for ZrO_2–SiO_2 materials, were used for the Si–O, Zr–O, O–O, Zr–Si, Si–Si and Zr–Zr atomic pairs, respectively. The amplitude of random atomic movements was initially 0.03 nm which was gradually reduced to 0.001 nm during the final stages of the simulation processes.

The probability of accepting an atomic movement was determined by comparing the model calculated with the experimental atomic distribution functions, $G(r)$, obtained from the present X-ray diffraction studies. Each of the particular simulation processes discussed below was terminated when approximately 10^5 atomic moves were completed and no further improvement of the fit to the experimental data could be achieved.

3.1. RMC simulations on the $0.5ZrO_2 \cdot 0.5SiO_2$ xerogel

Having established that the investigated xerogel samples are unlikely to be a mixture of ZrO_2 and SiO_2 phases we looked for structural models in which Zr and Si atoms are homogeneously distributed at the atomic level. For the $0.5ZrO_2 \cdot 0.5SiO_2$ xerogel a model based on the structure of crystalline $ZrSiO_4$ was investigated. For reference, crystalline $ZrSiO_4$ can be considered as an assembly of SiO_4 and ZrO_4 tetrahedra where no direct links between like (SiO_4 or ZrO_4) tetrahedral units exist [25]. A segment of the starting atomic configuration with the crystalline $ZrSiO_4$ structure is shown in Fig. 4. To ensure that the basic structural features of the starting atomic configuration do not become completely lost in the course of the simulation process and thus enable us to look for the presence of these features in the $0.5ZrO_2 \cdot 0.5SiO_2$ xerogel some extra constraints on the simulation process were imposed. It was required that the immediate oxygen co-ordination of Si and Zr atoms is

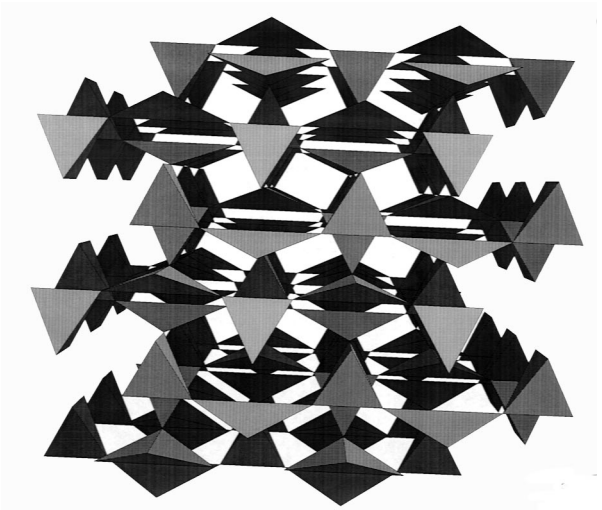

Figure 4 Segment of the initial atomic configuration used in the RMC simulations on the structure of the $0.5ZrO_2 \cdot 0.5\,SiO_2$ xerogel. The configuration is that of the structure of crystalline $ZrSiO_4$ [25] being a regular assembly of almost perfect SiO_4 and distorted ZrO_4 tetrahedra.

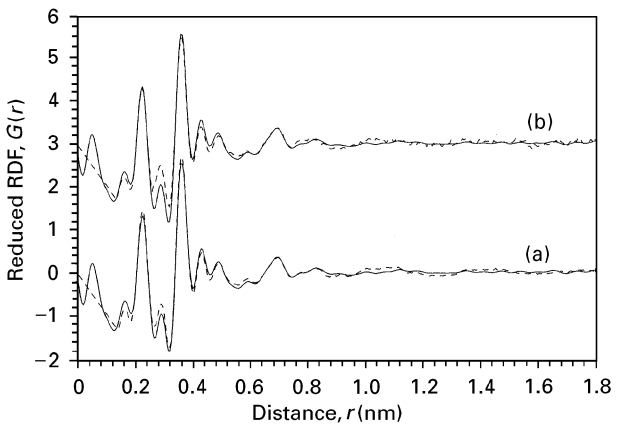

Figure 5 Comparison between (—) experimental and (- - -) model reduced atomic distribution functions for the $0.5ZrO_2 \cdot 0.5\,SiO_2$ xerogel. The model data shown in spectrum (a) are calculated from an atomic configuration initially having the structure of crystalline $ZrSiO_4$. The model data shown in spectrum (b) are calculated from an atomic configuration initially having the structure of crystalline $ZrSiO_4$ where, in addition, the positions of 10% of the Zr and Si atoms have been interchanged.

approximately preserved. Under these simulation conditions the starting atomic configuration rapidly relaxed to a state consistent with the experimental structural data for $0.5ZrO_2 \cdot 0.5SiO_2$ xerogel.

As can be seen in Fig. 5 (per spectrum (a)) a model based on the structure of crystalline $ZrSiO_4$ reproduces the experimental data for $0.5ZrO_2 \cdot 0.5SiO_2$ more closely than does a model based on a mixture of ZrO_2 and SiO_2 phases (see Fig. 3). This result of our simulations suggests that Zr and Si atoms in the $0.5ZrO_2 \cdot 0.5SiO_2$ xerogel are highly likely to be uniformly distributed at the atomic level in a way similar to that encountered in crystalline $ZrSiO_4$. However, since the experimental $G(r)$ peak amplitudes at 0.16 and 0.235 nm were not closely reproduced by this structural model we have attempted to further refine it. Initially we checked for the possible microclustering of Zr atoms that was suggested by the molecular dynamics simulations performed by Damodaran *et al.* [15]. To do so we randomly interchanged the atomic positions of 10% of the Si and Zr atoms in the model thus creating an atomic assembly containing first neighbour Zr–O–Zr and Si–O–Si local atomic configurations which, otherwise, do not occur in crystalline $ZrSiO_4$ and the initial RMC model. The modified structural model, however, produced an even greater discrepancy with the experimental data especially in the region around 0.28 nm (Spectrum (b) in Fig. 3), where according to our preliminary analyses on the experimental $G(r)$, the first neighbour Zr–Si atomic correlations occur. The observed discrepancies clearly indicated that first neighbour Zr–O–Zr and Si–O–Si atomic configurations are unlikely to exist in the $0.5ZrO_2 \cdot 0.5SiO_2$ investigated xerogel. In addition, our simulations do not support the results of Damodaran *et al.* [15] that suggested an inherent tendency of Zr atoms towards clustering in ZrO_2–SiO_2 gels.

Since this modification of the initially constructed RMC model turned out to be an unsuccessful one, another, more suitable modification was looked for. Recalling the fact that the ZrO_2–SiO_2 gels were obtained with a rather porous morphology and often showed a deviation from the targeted nominal chemical composition, we tried to refine the initial RMC model by eliminating a certain amount of Zr atoms from the model thereby simulating a non-stoichiometric, i.e., defect containing gel structure. The amount of Zr atoms (approximately 10%) we eliminated was suggested by the results of our detailed chemical analyses which showed that the actual chemical composition of the investigated xerogel is $0.5Zr_{1-\delta}O_2 \cdot 0.5SiO_2$ where $\delta = 0.1$. It should be noted that, most probably due to the specifics of the sol–gel preparation route, ZrO_2–SiO_2 gels have often been found to be slightly Zr deficient (see Table I in reference [14]). With this modification incorporated into the initial RMC model we were able to almost perfectly reproduce the experimental $G(r)$ data, for the xerogel with a nominal chemical composition of $0.5ZrO_2 \cdot 0.5SiO_2$, shown in Fig. 2. The modified structural model also closely reproduced the corresponding experimental $S(q)$ data shown in Fig. 1. The goodness-of-fit indicator in real space achieved with the model data in Fig. 2 is approximately 17%. For reference, this value is only approximately 3.5% when the corresponding pair atomic distribution functions, $g(r) = \rho(r)/\rho_0$, instead of the reduced atomic distribution functions are compared to each other.

3.2 RMC simulations on the $0.3ZrO_2 \cdot 0.7SiO_2$ xerogel

Since our preliminary analyses on the experimental structural data suggested that the $0.3ZrO_2 \cdot 0.7SiO_2$ xerogel is unlikely to be a mixture of ZrO_2 and SiO_2 phases a model assuming a homogeneous distribution of Zr and Si atoms was looked for. Considering the success of the RMC model based on the structure of crystalline $ZrSiO_4$ in approximating the atomic

arrangement in the $0.5ZrO_2 \cdot 0.5SiO_2$ xerogel we decided to adapt the final atomic configuration corresponding to this model to the case of the $0.3ZrO_2 \cdot 0.7SiO_2$ xerogel. To do so we substituted Zr atoms for Si atoms in the model atomic configuration so as to satisfy the findings of our detailed chemical analyses that showed that the actual chemical composition of the investigated xerogel is $0.3Zr_{1-\delta}O_2 \cdot 0.7SiO_2$, where $\delta = 0.11$. This model, assuming a uniform distribution of Zr–O polyhedra in a matrix of Si–O polyhedra, did reasonably well in reproducing the experimental structural data for the investigated xerogel shown in Figs 1 and 2. The goodness-of-fit indicator achieved in real space with the model data in Fig. 2 is approximately 19%. Again for reference, this value is only approximately 3.9% when the corresponding pair atomic distribution functions, $g(r) = \rho(r)/\rho_0$, instead of the reduced atomic distribution functions are compared to each other.

Given the good agreement observed between the present RMC simulations and the experimental structural data for $xZrO_2 \cdot (1-x)SiO_2$ xerogels ($x = 0.3$, 0.5) one may expect that the structural characteristics of the investigated materials are likely to be closely matched by the constructed three dimensional atomic configuration.

4. Discussion

The analysis of the present RMC structure models started with the derivation of the partial atomic distribution functions, $G_{ij}(r)$, $(i,j = Zr, Si, O)$. The partial atomic distribution functions for the $0.5ZrO_2 \cdot 0.5SiO_2$ xerogel are shown in Fig. 6 (a and b) and those for $0.3ZrO_2 \cdot 0.7\,SiO_2$ in Fig. 7 (a and b). As can be seen in the figures the atomic partial distribution functions that contain oxygen are quite similar for both investigated xerogels. Both $G_{O-O}(r)$ partial functions have only one well defined peak at 0.22 nm indicating the presence of only short-range order correlations between O atoms in both xerogels. Both $G_{Si-O}(r)$ functions have a large amplitude first peak at 0.163 nm, a second one at 0.23 nm and subsequent hardly discernible oscillations extending up to 1.8 nm.

In both $G_{Zr-O}(r)$ functions the first peak is split into two components at 0.203 and 0.23 nm with other peaks being positioned at approximately 0.4, 0.65, 0.88, 1.22 and 1.6 nm. The splitting of the first peak into two components in both $G_{Zr-O}(r)$ functions suggests that there are two distinct Zr–O first neighbour distances in the investigated xerogels. It is interesting to note that recent EXAFS experiments have also found two distinct Zr–O distances in the first co-ordination shell of Zr atoms in ZrO_2–SiO_2 xerogels [14]. The shorter Zr–O distance at approximately 0.203 nm has been attributed to bridging Zr–O–Si bonds while the longer Zr–O distance at approximately 0.23 nm to terminal (non-bridging) Zr–O bonds. We consider that the good agreement between the predictions of the present RMC models and the experimental EXAFS findings is strong evidence supporting the reliability of our simulations.

As can be seen in Figs 6 (a) and 7 (a) Zr–Zr atomic distribution functions for both the investigated

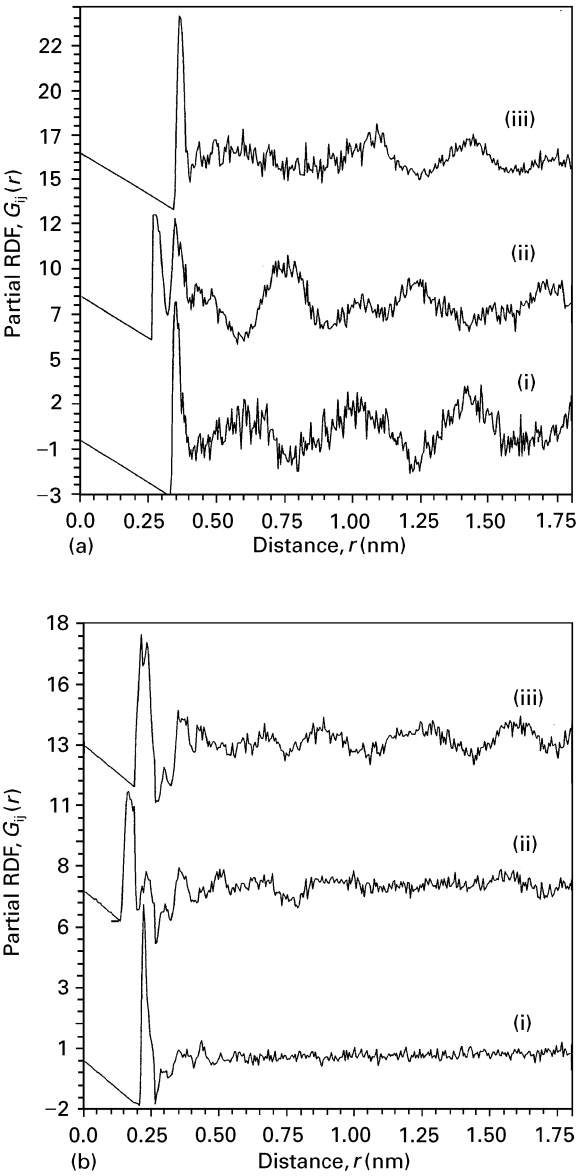

Figure 6 Partial atomic distribution functions, $G_{ij}(r)$, for the $0.5ZrO_2 \cdot 0.5\,SiO_2$ xerogel according to the present RMC simulations: (a) (i) Si–Si, (ii) Si–Zr and (iii) Zr–Zr and (b) (i) O–O, (ii) Si–O and (iii) Zr–O.

xerogels are also quite similar. They are characterized by a dominant peak at 0.365 nm and two more distant oscillations positioned at approximately 1.1 and 1.43 nm. Since there are no Zr atoms separated by distances less than 0.365 nm, which is the first neighbour Zr–Zr distance occurring in crystalline $ZrSiO_4$, one may assume that, similarly to the corresponding crystal, Zr atoms in the investigated $0.5ZrO_2 \cdot 0.5\,SiO_2$ xerogel sample are uniformly distributed at the atomic scale. The same assumption also holds for the $0.3ZrO_2 \cdot SiO_2$ xerogel since the Zr–Zr atomic correlations observed in this case are similar to those found in the structural model for the $0.5ZrO_2 \cdot 0.5\,SiO_2$ xerogel.

As one can see in Figs 6 (a) and 7 (a) according to the present simulations Zr–Si atomic distribution functions in $xZrO_2 \cdot (1-x)\,SiO_2$ xerogels ($x = 0.3, 0.5$) also exhibit similar features. Both $G_{Zr-Si}(r)$ functions have two pronounced peaks at 0.27 and 0.36 nm followed by small amplitude oscillations

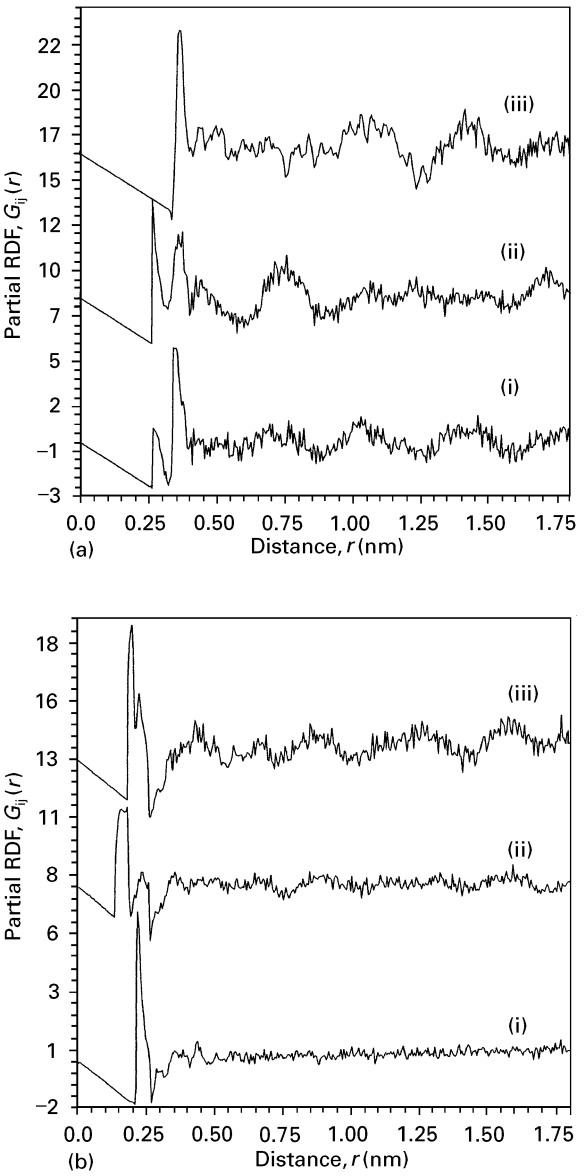

Figure 7 Partial atomic distribution functions, $G_{ij}(r)$, for the $0.3ZrO_2 \cdot 0.7\,SiO_2$ xerogel according to the present RMC simulations: (a) (i) Si–Si, (ii) Si–Zr and (iii) Zr–Zr and (b) (i) O–O, (ii) Si–O and (iii) Zr–O.

positioned at 0.75, 1.03, 1.23 and 1.7 nm. As may be expected the long-range (above approximately 0.5 nm) Zr–Si atomic correlations in the $0.3ZrO_2 \cdot 0.7\,SiO_2$ xerogel, where the Zr concentration is much less than the Si one, are weaker than these found in the $0.5ZrO_2 \cdot 0.5\,SiO_2$ xerogel, where Zr and Si species approximately have the same atomic concentration. It should be noted that the first peak in both $G_{Zr-Si}(r)$ functions at approximately 0.285 nm, which is close to the first neighbour Zr–O–Si atomic distance in crystalline $ZrSiO_4$, evidently reflects Zr–O–Si atomic configurations in the present structure models for the investigated $xZrO_2 \cdot (1-x)\,SiO_2$ xerogels ($x = 0.3,\ 0.5$). The presence of such Zr–O–Si configurations (Zr–O–Si bonds) in ZrO_2–SiO_2 amorphous materials has also been observed in several spectroscopic experiments [8, 9, 13, 14].

According to the present RMC simulations the Si–Si atomic distribution function for the $0.5ZrO_2 \cdot 0.5\,SiO_2$ xerogel has a first well defined peak at 0.35 nm followed by much broader ones at 0.65, 1.02 and 1.43 nm. The position of the first peak corresponds to the first neighbour Si–Si interatomic distances in crystalline $ZrSiO_4$. Therefore, one may well assume that, similar to the corresponding crystal, the distribution of Si atoms in the investigated $0.5ZrO_2 \cdot 0.5\,SiO_2$ xerogel is more or less uniform. However, as one can see in Fig. 7 (a) the Si–Si atomic correlation function for $0.3ZrO_2 \cdot 0.7\,SiO_2$ xerogel has two well defined peaks at approximately 0.28 and 0.35 nm in addition to the small amplitude oscillations positioned at approximately 0.7, 1.05 and 1.43 nm. These two peaks indicate that there are two types of first neighbour Si–Si distances in the present structural model for the $0.3ZrO_2 \cdot 0.7\,SiO_2$ xerogel. The longer of these Si–Si distances (0.35 nm) may, as in the case of the $0.5ZrO_2 \cdot 0.5\,SiO_2$ xerogel, be attributed to Si–Si pairs mediated by Zr–O polyhedral units. The shorter one (0.28 nm) then may be attributed to Si–Si pairs not mediated by such polyhedra. The emergence of more closely spaced Si–Si atomic pairs in the $0.3ZrO_2 \cdot 0.7\,SiO_2$ xerogel, suggested by the results of the present simulations, is not surprising considering the relatively high Si atomic species content present in this material. It should be noted that the results of the molecular dynamics simulations of Damodaran *et al.* [15] also suggest the presence of relatively closely spaced Si atoms, occupying the centres of linked Si–O polyhedra, in the gels with the composition of $0.3ZrO_2 \cdot 0.7\,SiO_2$.

Other important characteristics of the local atomic arrangement in the investigated xerogels obtained from the RMC models were the partial co-ordination numbers. These were obtained by counting all atomic pairs falling into co-ordination shells with boundaries of 0.235, 0.265, 0.290, 0.345, 0.410 and 0.42 nm for the Si–O, O–O, Zr–O, Zr–Si, Zr–Zr and Si–Si atomic pairs, respectively. The boundaries of the co-ordination shells were considered to coincide with the minima following the first well defined peaks in the corresponding partial atomic distribution functions. The partial co-ordination numbers obtained in this study are summarized in Table I. As can be seen in the table the first co-ordination numbers for Si–O from the present structural models are close to 4 indicating the presence of SiO_4 tetrahedral units in both of the investigated xerogel samples. This inference is also supported by the fact that the first neighbour O–O distance found ($r_{O-O} = 0.22$ nm) is close to $2(2/3)^{1/2}\, r_{Si-O}$ ($r_{Si-O} = 0.163$ nm) as it should be with tetrahedral SiO_4 co-ordination units. Since the O–Si first co-ordination number in the $0.5ZrO_2 \cdot 0.5\,SiO_2$ xerogel is close to 1 there are obviously no coupled SiO_4 tetrahedra in this material. In the $0.3ZrO_2 \cdot 0.7\,SiO_2$ xerogel, where the O–Si first co-ordination number is greater than 1, then coupled SiO_4 units are very likely to occur. In both investigated xerogels the Zr–O first co-ordination number is close to 5 which is well in line with the results of several reported spectroscopic studies [14 and references therein] as well with the predictions of the molecular dynamics simulations of Damodaran *et al.* [15]. We consider that the close agreement between the present findings and the results

TABLE I Partial co-ordination numbers, for $xZrO_2 \cdot (1-x)\,SiO_2$ xerogels (x = 0.3, 0.5) calculated using the RMC structural models developed in this work

	$0.5ZrO_2 \cdot 0.5SiO_2$	$0.3ZrO_2 \cdot 0.7SiO_2$
Si–O	3.81	3.75
O–Si	0.96	1.3
O–Zr	1.05	0.82
Zr–O	5.28	5.07
Zr–Si	2.20	2.30
Si–Zr	3.45	1.07
Zr–Zr	2.48	1.65
Si–Si	3.12	5.23
O–O	3.87	3.74

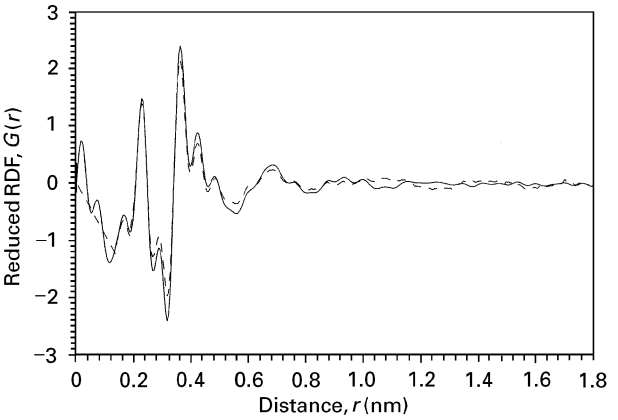

Figure 8 Reduced atomic distribution function, $G(r)$, for the $0.5ZrO_2 \cdot 0.5\,SiO_2$ xerogel thermally treated at 770 K. Key: (—) experimental data, (- - -) RMC fit.

of previous investigations as further evidence in support of the reliability of the performed RMC simulations.

Considering that the O–Zr first co-ordination numbers in the present structural models have been found to be close to unity, one may well assume that no coupled Zr–O polyhedral units occur in the investigated xerogel materials. The proposed uniform distribution of the Zr atoms (Zr–O polyhedra) in the $xZrO_2 \cdot (1-x)\,SiO_2$ xerogels (x = 0.3, 0.5) is supported by the fact that no change in the Zr–Si first co-ordination number is observed with the change in the relative amount of Zr and Si atomic species (see Table 1). Some changes in the number of first Si–Zr and Zr–Zr neighbours, in line with the change in the relative content of Si and Zr atomic species, are, however, predicted by the results of the present simulations. As one may expect with the increase of the relative amount of Si atomic species the number of first Si–Zr and Zr–Zr atomic neighbours decreases and that of the Si–Si atomic neighbours increases (see Table I).

In general, the results of the present simulations suggest that at the atomic scale $xZrO_2 \cdot (1-x)\,SiO_2$ xerogels (x = 0.3, 0.5) may be considered to be an assembly of irregular Zr–O polyhedra, involving short (0.203 nm) and long (0.23 nm) Zr–O bonds, uniformly imbedded into a matrix of SiO_4 tetrahedral units. In particular, this specific atomic arrangement in the $0.5ZrO_2 \cdot 0.5\,SiO_2$ xerogel is closely related to that in crystalline $ZrSiO_4$.

The question as to: why do ZrO_2–SiO_2 xerogels, in which, according to the results of the present simulations, Zr and Si atoms are homogeneously distributed at the atomic level, always decompose into Zr and Si rich phases upon prolonged thermal treatment at elevated temperatures? arises. To address this question it was necessary to perform some extra investigations. A sample of the $0.5ZrO_2 \cdot 0.5\,SiO_2$ xerogel was further thermally treated at 770 K for 4 h and then investigated by X-ray diffraction. The experimental atomic distribution function obtained in the same manner as previously discussed is shown in Fig. 8. A comparison between the experimental atomic distribution functions for the sample that did not receive an extra heat treatment (Fig. 2) and the sample treated at 770 K (Fig. 8) shows that they are rather similar and obviously both correspond to samples in an amorphous state. Given the similarity of both sets of experimental data we tried to fit the data for the further thermally treated sample with the RMC structural model that reproduced the data for the standard thermally treated sample. The model is able to reproduce the experimental results shown in Fig. 8. An analysis of the calculated model atomic configuration showed that its characteristics were not very different from those of the initial one with small differences being observed in the Si–O first, Si–Si second and Zr–Zr second co-ordination numbers. For the sample that received the extra thermal treatment all these co-ordination numbers were found to be slightly higher than the corresponding ones for the standard xerogel. This indicates that some kind of densification of the atomic arrangement occured on further thermal treatment but that the main characteristics of the xerogel, including the distribution of Zr and Si atoms, remained unchanged. Thus these results indicated that up to the point where the first indications of crystallization are observed the atomic scale structure of the $0.5ZrO_2 \cdot 5\,SiO_2$ xerogel is not substantially changed and, as indicated by the results of the present simulations, it is highly likely to be an assembly of uniformly distributed Zr–O and Si–O polyhedra.

In this way our studies suggest that a separation into Zr and Si rich phases takes place only upon a crystallization of $xZrO_2 \cdot SiO_2$ xerogels (x = 0.3, 0.5), which in our case occurs at temperatures slightly above 770 K, and that this crystallization is most probably due to an increased diffusion promoted by the thermal inpact and it is not due to the presence of some initial Zr and/or Si microsegregation. It is interesting to note that ZrO_2–SiO_2 glasses [8] and even $ZrSiO_4$ crystals [25], have also been found to be unstable against thermal treatment decomposing into Si rich and Zr rich phases at temperatures higher than 1000 K. In this respect, it seems that in the ZrO_2–SiO_2 xerogels this phase decomposition occurs at slightly lower temperatures (770–800 K) which is probably due to the greater degree of structural disorder already present in them.

5. Conclusions

The results of the present X-ray diffraction and RMC studies suggest that at the atomic level $xZrO_2 \cdot (1 - x)$ SiO_2 xerogels ($x = 0.3, 0.5$) are highly likely to be an assembly of uniformly distributed Zr–O and Si–O polyhedral units. The reason for the homogeneous distribution of Si and Zr atomic species in the investigated xerogels could lie in the specifics of the sol–gel process employed in their preparation, namely, in the intimate mixing of Si and Zr alkoxide components in the sol precursor achieved by a careful control on the sol formation rate. Thus the results of the present study clearly demonstrate the success of the sol–gel method in yielding ZrO_2–SiO_2 amorphous materials with a homogeneous microstructure whose basic characteristics are preserved even after a prolonged thermal treatment at 770 K.

Acknowledgements

An Alexander von Humboldt Research Fellowship is gratefully acknowledged by one of the authors (VP). The work was supported by Deutsche Forschungsgemeinschaft (Grant Ge 667/3-1).

References

1. M. ANAST, J. BELL, T. BELL and B. BEN-NISSAN, *J. Mater. Sci.* **11** (1992) 1483.
2. M. ATIK and M. AEGERTER, *J. Non-Cryst. Solids* **147–148** (1992) 813.
3. R. SIMHAN, *ibid.* **54** (1983) 335.
4. B. YOLDAS, *ibid.* **38–39** (1980) 81.
5. T. OSUKA, H. MORIKAWA, F. MARUMOTO, K. TOHJI, Y. UDAGAWA, A. YASUMORI and M. YAMANE, *ibid* **82** (1986) 154.
6. M. NOGAMI, *J. Mater. Sci.* **21** (1986) 3513.
7. S. SAHA and P. PRAMANIK, *J. Non-Cryst. Solids* **159** (1993) 31.
8. I. SALVADO, C. SERNA and F. NAVARRO, *ibid.* **100** (1988) 330.
9. T. SUGAMA, N. CARCIELLO and M. MIURA, *Thin Solid Films* **216** (1992) 249.
10. M. SALVADO and F. NAVARRO, in Proceedings of the XVI Congress on Glass, Madrid, 1992 published as special issue of *Bull. Soc. Esp. Ceram. V.D.* **31-C** (1992) 251.
11. Y. KANNO, *J. Mater. Sci. Lett.* **9** (1990) 765.
12. M. PALLADINO, F. PIRINI, M. BEGHI, P. CHIURLO, G. COGLIATI and L. COSTA, *J. Non-Cryst. Solids* **147–148** (1992) 335.
13. S. LEE and R. CONDRATE, *J. Mater. Sci.* **23** (1988) 2951.
14. K. OKASAKA, H. NASU and K. KAMIYA, *J. Non-Cryst. Solids* **136** (1991) 103.
15. K. DAMODARAN, V. NAGARAJAN and K. RAO, *ibid.* **124** (1990) 233.
16. Th. GERBER, B. HIMMEL, *J. de Phys* IV France, Coll. C8, **3** (1993) 585.
17. Th. GERBER, B. HIMMEL, U. BUTTLER, H. BÜRGER and U. BRÄUTIGAM, Eur. Mater. Res. Soc. Monogr. Vol. 5 (EMRS. 1992) p. 431.
18. H. KLUG and L. ALEXANDER, in "X-ray diffraction procedures for polycrystalline and amorphous materials" (Wiley, New York, 1974).
19. F. HAJDU, *Acta Cryst.* **A28** (1972) 250.
20. A. THAKKAR and D. CHAPMAN, *ibid.* **A31** (1975) 391.
21. R. McGREEVY and L. PUSZTAI, *Mol. Simul.* **1** (1988) 359.
22. R. McGREEVY, *J. Phys.: Condens. Matter* **3** (1991) F9.
23. R. McGREEVY, M. HOVE, D. KEEN and K. KLAUSEN, in "Neutron scattering Data Analysis" (Inst. Phys. Conf. Proc. Ser. 107) (Institute of Physics, Bristol, 1989 p. 165).
24. A. BARANYAI, A. GEIGER, P. CARTRELL-KILLS, K. HEINZERGER, R. MCGREEVY, G. PALINCAS and I. RUFF, *J. Chem. Soc. Faraday Trans.* **83** (1987) 1335.
25. Z. MURZIC, T. VOGT and F. FREY, *Acta Cryst.* **B48** (1992) 584.

Received 5 June 1996
and accepted 10 February 1997